DEAD-box protein family member DDX28 is a negative regulator of HIF-2α and eIF4E2-directed hypoxic translation

Sonia L. Evagelou[1], Olivia Bebenek[1], Erin J. Specker[1], James Uniacke[1,*]

[1]Department of Molecular and Cellular Biology, University of Guelph, 50 Stone Road East, Guelph, Ontario, Canada, N1G 2W1

***Corresponding author:**
James Uniacke: Department of Molecular and Cellular Biology, University of Guelph, 50 Stone Road East, Guelph, Ontario, Canada N1G 2W1; juniacke@uoguelph.ca; Tel.: 519-824-4120 ext. 54739

RUNNING TITLE: DDX28 negatively regulates HIF-2α

Abbreviations: BrdU, bromodeoxyuridine; CCRCC, clear cell renal cell carcinoma; DDX28, DEAD box protein 28; EEF2, Eukaryotic Translation Elongation Factor 2; EGFR, Epidermal Growth Factor Receptor; eIF4E, eukaryotic initiation factor 4E; HIF, Hypoxia-inducible factor HSP90ab1, Heat Shock Protein 90 Alpha Family Class B Member 1; IGF1R, Insulin Like Growth Factor 1 Receptor; PEI, polyethylenamine; rHRE, RNA Hypoxia Response Elements

Keywords: Translation, hypoxia, HIF, DEAD-box protein, oxygen, eIF4E2

Conflict of interest: The authors declare that they have no conflicts of interest with the contents of this article.

ABSTRACT

Hypoxia occurs when there is a deficiency in oxygen delivery to tissues and is connected to physiological and pathophysiological processes such as embryonic development, wound healing, heart disease and cancer. The master regulators of oxygen homeostasis in mammalian cells are the heterodimeric hypoxia-inducible transcription factors HIF-1 and HIF-2. The oxygen-labile HIF-2α subunit has not only been implicated in transcription, but also as a regulator of eIF4E2-directed hypoxic translation. Here, we have identified the DEAD-box protein family member DDX28 as a novel interactor and negative regulator of HIF-2α that suppresses its ability to activate eIF4E2-directed translation. We demonstrate that stable silencing of DDX28 via shRNA in hypoxic human U87MG glioblastoma cells caused an increase, relative to control, to: HIF-2α protein levels, the ability of eIF4E2 to bind the m^7GTP cap structure, and the translation of select eIF4E2 target mRNAs. DDX28 depletion elevated both nuclear and cytoplasmic HIF-2α, but HIF-2α transcriptional activity did not increase possibly due to its already high nuclear abundance in hypoxic control cells. Depletion of DDX28 conferred a proliferative advantage to hypoxic, but not normoxic cells, which is likely a consequence of the translational upregulation of a subset of hypoxia-response mRNAs. DDX28 protein levels are reduced in several cancers, including glioma, relative to normal tissue. Therefore, we uncover a regulatory mechanism for this potential tumor suppressor in the repression of HIF-2α- and eIF4E2-mediated translation activation of oncogenic mRNAs.

INTRODUCTION

The procurement for oxygen is a fundamental aspect of survival for aerobic organisms in all domains of life. Mammals have evolved complex circulatory, respiratory, and neuroendocrine systems to satisfy the need for molecular oxygen as the primary electron acceptor in oxidative phosphorylation, which supplies energy in the form of ATP [1]. The ability of a cell to acclimate to low oxygen (hypoxia or $\leq$ 1% O_2), which usually arises due to an imbalance in supply and demand, is essential from the earliest stages of life [2, 3]. Hypoxia plays a role in several physiological and pathophysiological conditions such as embryonic development, muscle exercise, wound healing, cancer, heart disease, and stroke [4]. Prior to the establishment of uteroplacental circulation, embryonic cells receive only as much as 2% O_2, and following oxygenation by maternal blood, the embryo still contains discrete regions of hypoxia [2, 5]. This form of physiological hypoxia helps govern the process of development through cell fate determination, angiogenesis, placentation, cardiogenesis, bone formation, and adipogenesis [3, 6-10]. Hypoxia is also a feature of the tumor microenvironment, and plays a key role in several cancer hallmarks toward tumor progression [11, 12]. The major cellular response to hypoxia is mediated by hypoxia-inducible transcription factors (HIF-1 and HIF-2). The HIFs are heterodimeric, composed of an oxygen-labile α-subunit, HIF-1α or HIF-2α, and a constitutively expressed HIF-1β subunit [11]. HIF-1 and HIF-2 activate the transcription of hundreds of genes (some shared and some unique), including those involved in metabolism and erythropoiesis, in order to simultaneously reduce the activity of energy-expensive processes and promote the increased uptake of nutrients and oxygen [13]. Further investigation into the unique roles of HIF-1α and HIF-2α, and how they might be differentially regulated, will reveal novel insights into hypoxic gene expression.

Unlike HIF-1α that is more involved in acute hypoxia (< 24 h), HIF-2α is linked to chronic hypoxia [14]. Further, HIF-2α accumulates in both the cytoplasm and the nucleus [15]. Indeed, HIF-2α, but not HIF-1α, participates in the recruitment of select hypoxia-response mRNAs to the translation apparatus [16], not only in hypoxia but in the low-range of physiological oxygen (< 8% O_2) [17]. Hypoxia is a potent inhibitor of mammalian target of rapamycin complex 1, suppressing canonical cap-dependent translation by sequestering the cap-binding protein eukaryotic initiation factor 4E (eIF4E) [18-21]. Alternative modes of translation initiation are utilized during hypoxia including cap-independent mechanisms as well as non-canonical cap-dependent translation mediated by the eIF4E2 cap-binding protein. HIF-2α and RBM4 recognize select mRNAs by binding to RNA Hypoxia Response Elements (rHREs) in their 3' UTRs and initiating their translation via the 5' cap through eIF4E2, eIF4G3 and eIF4A [16, 22]. HIF-2α and eIF4E2 are essential for embryonic development [3, 23], and important contributors to tumor progression [24, 25], both hypoxia-driven processes. The protein levels of eIF4E2 do not change between normoxia and hypoxia [16, 17]. HIF-2α, on the other hand, is constantly degraded in normoxia via a family of prolyl hydroxylases that are inhibited by hypoxia [11]. In hypoxia, it is mostly unclear how the activities of eIF4E2 or HIF-2α are regulated with respect to translation initiation. A greater understanding of these mechanisms will shed light on how gene expression is coordinated in physiological and pathophysiological processes that are linked to hypoxia.

Here we demonstrate that the DEAD box protein DDX28 is a negative regulator of HIF-2α protein levels in a human glioblastoma cell line. DDX28 has been detected in mitochondria, cytoplasm and nuclei [26]. However, known functions of DDX28 are limited to its RNAi-mediated silencing disrupting mitoribosome assembly [27, 28], which is also an outcome of

hypoxia [29]. While it is known that hypoxia increases HIF-2α levels, our data show that DDX28 protein levels concurrently decrease. We also show that DDX28 interacts with HIF-2α, but not HIF-1α or the m^7GTP cap structure. We demonstrate a link between these two observations by depleting DDX28 levels in hypoxia whereby an even greater increase to HIF-2α levels was observed along with its effect on eIF4E2-dependent translation activation. Hypoxic depletion of DDX28 caused eIF4E2 and its mRNA targets to associate more with the m^7GTP cap structure and polysomes, respectively. Furthermore, hypoxic depletion of DDX28 caused a significant increase to cell proliferation only in hypoxia. While HIF-2α increased in both the nucleus and cytoplasm upon DDX28 depletion, there was no increase to its transcriptional activity. We propose a model where DDX28 reduction in hypoxia plays a role in HIF-2α stabilization, but some DDX28 is still useful to restrain the HIF-2α/eIF4E2 translational axis, which can be oncogenic [24, 25].

RESULTS

DDX28 interacts with HIF-2α, but not HIF-1α or eIF4E2

U87MG human glioblastoma cells were used in this study because they have previously been characterized as models for hypoxia research and the interaction between HIF-2α and eIF4E2 in non-canonical cap-dependent translation [16, 17, 22, 24, 25]. When U87MG were exposed to hypoxia (1% O_2) for 24 h, we not only observed an increase in HIF-2α, but a concurrent decrease in DDX28 levels (Fig. 1A). Furthermore, when DDX28 was stably depleted via two independent shRNA sequences to produce two unique cell lines, the hypoxia-dependent increase in HIF-2α was further increased relative to controls expressing a non-targeting shRNA (Fig. 1B). We next investigated whether DDX28 was directly involved in HIF-2α regulation by performing a co-immunoprecipitation. Exogenous tagged proteins were used due to the lack of specificity of

the antibodies for the endogenous protein or its low abundance. In hypoxic U87MG cells, exogenous GFP-HIF-2α, but not GFP alone, co-immunoprecipitated with DDX28 (Fig. 1C). Since HIF-2α is a known interactor of eIF4E2 at the 5' mRNA cap in hypoxia [16], we tested whether DDX28 was part of this complex. However, exogenous eIF4E2 co-immunoprecipitated with HIF-2α, but not DDX28 (Fig. 1D). Further, to demonstrate specificity for the HIF-2α homolog, HIF-1α did not co-immunoprecipitate with DDX28 (Fig. 1E). These data suggest that DDX28 interacts with a distinct pool of HIF-2α that is not associated with eIF4E2.

Depletion of DDX28 enhances the association of eIF4E2 with m^7GTP and polyribosomes

We performed m^7GTP cap-binding assays to test whether the increased HIF-2α levels in DDX28 depleted cells had an effect on the translation initiation potential of eIF4E2. In hypoxia, eIF4E2 bound more to m^7GTP by 1.6 ± 0.1 and 1.5 ± 0.2 fold in two DDX28 depleted cell lines relative to control (Fig. 2A-B). Surprisingly, depletion of DDX28 in normoxia had an even greater effect on eIF4E2 binding to m^7GTP with 2.9 ± 0.4 and 2.5 ± 0.1 fold increases relative to control (Fig. 2C-D). These data are also in support of Fig. 1D that DDX28 does not bind the m^7GTP cap.

m^7GTP association of a cap-binding protein like eIF4E2 does not necessarily imply an increase in translation initiation [30]. Therefore we performed polysome fractionation to test whether eIF4E2 had a greater association with polysomes isolated from DDX28 depleted cells relative to controls in normoxia and hypoxia. Using densitometry to quantify total eIF4E2 associated with monosomes (low translation; fractions 1-3) and polysomes (medium to high translation; fractions 4-9), we show that 5 ± 1.2% of total eIF4E2 in normoxic control cells was associated with polysomes (Fig. 3A). In DDX28-depleted cells, the proportion of polysome-associated eIF4E2 increased to 23 ± 3.2% (Fig. 3B). Hypoxic control cells displayed 22 ± 5.1% eIF4E2 associated with polysomes (Fig. 3C), an increase relative to normoxic control cells (5 ±

1.2%; Fig. 3A). Hypoxic DDX28-depleted cells had an even greater proportion of eIF4E2 associated with polysomes (41 ± 4.1%) relative to hypoxic control cells (Fig. 3D). The polysome association of the canonical cap-binding protein eIF4E did not change in any condition (Fig. 3E). Our data show that hypoxia, or knockdown of DDX28 in normoxia, increased the proportion of polysome-associated eIF4E2 relative to normoxic control cells (Fig. 3F). However, DDX28 depletion and hypoxia together significantly increased the polysome association of eIF4E2 relative to normoxic control cells (Fig. 3F).

Depletion of DDX28 increases the translation of eIF4E2 target transcripts in hypoxia

We performed qRT-PCR on monosome and polysome fractions in normoxia and hypoxia to measure the DDX28-dependent association of eIF4E2 and eIF4E target transcripts. We chose Epidermal Growth Factor Receptor (*EGFR*) and Insulin Like Growth Factor 1 Receptor (*IGF1R*) mRNAs, previously characterized as eIF4E2-dependent transcripts due to the presence of an rHRE in their 3' UTR [16, 17], and Eukaryotic Translation Elongation Factor 2 (*EEF2*) and Heat Shock Protein 90 Alpha Family Class B Member 1 (*HSP90ab1*) mRNAs previously characterized as eIF4E-dependent transcripts due to the presence of a 5′ terminal oligopyrimidine motif [17, 31]. We observed a significant increase in the association of *EGFR* mRNA with polysomes relative to monosomes from 4.5 ± 0.9-fold in controls to 11.3 ± 1.6-fold in DDX28 depleted cells in hypoxia (Fig. 4A). Similarly, the polysome association of *IGF1R* mRNA significantly increased from 3.2 ± 0.3 in controls to 5.4 ± 0.7 in DDX28-depleted cells in hypoxia (Fig. 4A). In normoxia, there was no difference in the polysome-association of *EGFR* mRNA relative to monosomes between controls (3.5 ± 0.5-fold) and DDX28 depleted cells (3.8 ± 0.5-fold) (Fig. 4B). Similarly, there was no statistical difference in the polysome-association of *IGF1R* mRNA relative to monosomes between controls (5.6 ± 0.8-fold) and DDX28 depleted

cells (3.5 ± 0.5-fold) (Fig. 4B). Moreover, EGFR protein levels (Fig. 4C), but not total *EGFR* mRNA levels (Fig. 4D), increased in hypoxic DDX28-depleted cells relative to control. Neither of the eIF4E-dependent transcripts displayed significant changes in polysome-association in normoxia or hypoxia between DDX28-depleted and controls. The one exception was *EEF2* mRNA, which displayed a small significant increase in normoxic polysome-association relative to monosomes in DDX28-depleted cells (1.52 ± 0.04) compared to controls (1.05 ± 0.06) (Fig. 4E). These data suggest that DDX28 depletion significantly increases the translation of eIF4E2-dependent, but not eIF4E-dependent, transcripts in hypoxia.

Depletion of DDX28 in hypoxia increases cytoplasmic and nuclear HIF-2α levels, but not its nuclear activity

Hypoxic cells were fractionated into cytoplasm and nuclei to measure the effects of DDX28 depletion on HIF-2α levels in both compartments. In accordance with the abovementioned observations that DDX28 depletion increases total HIF-2α protein levels and its cytoplasmic activity (translation), we show that DDX28 depletion increased cytoplasmic HIF-2α levels compared to control (Fig. 5A). However, we also observed an increase in the nuclear levels of HIF-2α. Therefore, we investigated whether DDX28 depletion in hypoxia also increased the nuclear activity of HIF-2α (transcription) by measuring the mRNA abundance from its gene targets relative to control. We chose six genes that contain Hypoxia Response Elements in their promoters that are more dependent on HIF-2α than HIF-1α [32-35]. None of the six genes displayed a significant increase in mRNA abundance in DDX28 depleted cells relative to control (Fig. 5B). In fact, two genes displayed significant decreases in mRNA abundance, albeit by two-fold at most. These data suggest that while both nuclear and cytoplasmic HIF-2α levels increase in response to DDX28 depletion, the effect on HIF-2α transcriptional activity is minimal.

DDX28 depletion causes an increase in cell viability and proliferation in hypoxia but not normoxia

We next investigated whether the increase in eIF4E2-directed translation in DDX28 depleted cells provided a benefit to cells by measuring their viability and proliferation in normoxia and hypoxia. To assess this, we monitored the number of viable DDX28 depleted and control cells over 72 h at 24 h intervals using crystal violet staining. We observed no significant differences in viability at 24, 48, or 72 h between normoxic DDX28 depleted and control cells (Fig. 6A). However, both hypoxic DDX28 depleted cell lines had significantly increased viability compared to control at each time interval (Fig. 6B). To measure proliferation, we monitored the incorporation of bromodeoxyuridine (BrdU) into the DNA of actively dividing cells via immunofluorescence. In normoxia, one DDX28 depleted cell line displayed a significant increase in BrdU incorporation relative to control (Fig. 6C). However, following 24 h of hypoxia, both DDX28 depleted cell lines displayed significant increases in BrdU incorporation relative to control (Fig. 6D). To test whether overexpressing exogenous DDX28 would have the opposite effect (decreased viability, proliferation, and HIF-2α levels) in hypoxia, we generated two stable clonal U87MG cell lines expressing FLAG-DDX28 and a control expressing FLAG alone. We did not observe any significant differences in viability, proliferation, or HIF-2α levels between the overexpressing cell lines relative to the control (Fig. S1A-E). The one exception was a decrease in viability after 24 h of hypoxia in one of the overexpressing cell lines relative to control, but this difference ceased at 48 h and 72 h. Since hypoxia appears to reduce the levels of exogenous DDX28 (Fig. S1E), it is possible that the overexpressing cell lines do not overexpress DDX28 enough in hypoxia to suppress HIF-2α or that DDX28 is already suprastoichiometric to HIF-2α. Our data suggest that depletion of DDX28 provides an increase to cell viability and

proliferation in hypoxia likely through an increase in translation of select mRNAs and perhaps other unidentified pathways.

DISCUSSION

HIF-2α and eIF4E2 contribute to the ability of a cell to adapt to hypoxic conditions through selective gene expression by transcriptional and translation regulation. We have previously shown that eIF4E2 knockdown represses hypoxic cell proliferation and survival, migration and invasion, and tumor growth [24, 25]. Furthermore, eIF4E2-directed translation is active in the low range of physiological oxygen where HIF-2α, but not yet HIF-1α, is stabilized (3-8% O_2) [17]. Total levels of eIF4E2 protein are minimally altered upon hypoxic exposure [16, 17, 25, 36], so how is it regulated? Post-translational modifications of eIF4E2 have been identified such as ISGylation [37], as well as protein interactors such as eIF4G3 and eIF4A [16, 22]. However, the stabilization of HIF-2α is essential for eIF4E2 hypoxic activity [16] and is likely a more upstream regulatory step for eIF4E2-directed translation to be functional.

We have uncovered a new mode of HIF-2α regulation that affects the activity of hypoxic translation via eIF4E2. HIF-2α co-immunoprecipitated with DDX28 and eIF4E2 (Fig. 4C), but eIF4E2 did not co-immunoprecipitate with DDX28 (Fig. 4D). This suggests that DDX28 interacts with a different pool of HIF-2α than the one that interacts with eIF4E2. In agreement, DDX28 did not interact with the m^7GTP cap structure (Fig. 2). However, the depletion of DDX28 did significantly increase the ability of eIF4E2 to associate with m^7GTP, suggesting that its effect on HIF-2α influences eIF4E2 activity. Indeed, eIF4E2 did associate more with polysomes upon DDX28 depletion (Fig. 3F). Mechanisms were initially proposed where HIF-2α acted at the 3' UTR rHRE of select mRNAs along with RBM4 to mediate joining of the 5' end and eIF4E2 [16, 22, 38]. It is important to note that cap-binding assays are performed with

222 m^7GTP bound to agarose beads and not to an mRNA [39]. Therefore, these data suggest that
223 HIF-2α could act directly on eIF4E2 to regulate its cap-binding potential (Fig. 7).

224 While depletion of DDX28 significantly increased the ability of eIF4E2 to bind m^7GTP
225 in both normoxia and hypoxia, it was surprising that this increase was greater in normoxia than
226 in hypoxia (Fig. 2). This could indicate that DDX28 has increased relevance as a suppressor of
227 eIF4E2 activity in normoxia, but while the polysome-associated eIF4E2 increased in DDX28
228 depleted normoxic cells, it was not statistically significant (Fig. 3F). Further, the polysome
229 association of eIF4E2 mRNA targets *EGFR* and *IGF1R* did not increase in normoxic DDX28
230 depleted cells relative to control (Fig. 4B). In hypoxia, the effects of DDX28 depletion were not
231 only observed on eIF4E2 m^7GTP and polysome association, but here *EGFR* and *IGF1R* mRNAs
232 were significantly more associated with polysomes relative to control (Fig. 4A). We speculate
233 that depleting DDX28 in normoxia may increase the very low levels of HIF-2α to levels still
234 undetectable via western blot, but enough to significantly increase the cap-binding potential of
235 eIF4E2. The relative increase in HIF-2α in normoxic DDX28 depleted cells relative to control
236 may be greater than that in hypoxic cells, but there could be an unmet requirement in normoxia
237 for a threshold amount of total HIF-2α protein to efficiently activate eIF4E2 and the translation
238 of its mRNA targets. Unexpectedly, the increase in nuclear HIF-2α upon DDX28 depletion in
239 hypoxia did not produce subsequent increases to the transcription of its target genes (Fig. 5). We
240 speculate that perhaps in hypoxic control cells, the HIF-2α DNA binding sites are saturated.
241 Conversely, the cytoplasmic HIF-2α targets (i.e. eIF4E2, DDX28) are likely not saturated due to
242 the much lower levels of HIF-2α in this compartment relative to the nucleus.

243 Hypoxia decreases total DDX28 protein levels, but our data suggest that the remaining
244 DDX28 is important to restrain the HIF-2α/eIF4E2 translational axis. This brings into to question

why a negative regulator of this pathway would be in place, given that the expression of rHRE-containing mRNAs contributes to hypoxic survival [25]. Dozens of eIF4E2 mRNA targets have been identified such as *EGFR*, *IGF1R*, *PDGFRA*, *CDH22* [16, 17, 22, 24], and these have all been characterized as oncogenes [24, 40, 41]. Therefore, while important for hypoxic adaptation, tight regulation of this pathway is likely required to prevent neoplastic transformation. Indeed, mining the data in The Pathology Atlas within The Human Protein Atlas, we found that DDX28 is present in most tissues, but lost in the majority of cancers ($n \geq 3$ patients per cancer type; available from v18.proteinatlas.org and https://www.proteinatlas.org/ENSG00000182810-DDX28/pathology) [42]. Conversely, the presence of DDX28 is listed as a favorable prognostic marker in cases of renal cell carcinoma. More than 80% of all clear cell renal cell carcinomas (CCRCC), the most common form of renal cancer, contain inactivating mutations in the *VHL* gene that stabilize the HIF-α subunits in a hypoxia-independent manner [43]. The normoxic stabilization of HIF-2α and activation of its oncogenic pathways that occurs in CCRCC could be antagonized by the presence of DDX28. This study was performed in U87MG glioblastoma cells, but since DDX28 appears to be expressed ubiquitously, it could function similarly in other tissues. We provide mechanistic insight into the regulation of HIF-2α and eIF4E2-directed hypoxic translation, and support for DDX28 as a tumor suppressor and prognostic marker to deepen our understanding of cancer progression.

METHODS

Cell Culture

U87MG human glioblastoma cells (HTB-14) were obtained from the American Type Culture Collection and maintained as suggested. Normoxic cells were maintained at 37 °C in ambient O_2 levels (21%) and 5% CO_2 in a humidified incubator. Hypoxia was induced by culturing at 1% O_2

and 5% CO_2 at 37 °C for 24 h, unless otherwise stated, using an N_2-balanced Whitley H35 HypOxystation.

Generation of Stable Cell Lines

Two unique OmicsLink™ shRNA expression vectors (Genecopoeia) were used to target the coding sequence of human DDX28 [HSH014712-3-nU6 sequence 5'-ggtggactacatcttagag-3', HSH014712-3-nU6 sequence 5'-acgctgcaagattacatcc-3']. A non-targeting shRNA was used as a control. U87MG cells stably expressing C-terminal 3x FLAG tagged DDX28 were generated by transfecting cells with the OmicsLink™ pEZ-M14 EX-A3144-M14 expression vector encoding the human DDX28 coding sequence (Genecopoeia). Selection was initiated 48 h post-transfection using 1 μg/mL puromycin or 400 μg/mL G418, respectively, and single colonies were picked after seven days.

Western Blot analysis

Standard western blot protocols were used. Primary antibodies: anti-eIF4E2 (Genetex, GTX82524), anti-DDX28 (Abcam, ab70821), anti-eIF4E (Cell Signaling, C46H6) anti-GAPDH (Cell Signaling, D16H11), anti-RPL5 (Abcam, ab137617), anti-HIF-2α (Novus, NB100-122), anti-FLAG (Sigma, F1804), anti-α-tubulin (GeneTex, GT114), anti-lamin a/c (Cell Signaling, 2032), anti-GFP (Abcam, ab290), anti-HA (Santa Cruz, Y-11), anti-β-Actin (Genetex, GT5512), and anti-EGFR (Proteintech, 18986-1-AP).

Polysome Profiling and analysis

Performed as described previously [17]. The total eIF4E2 or eIF4E signal was quantified by densitometry using Bio-Rad Image Lab software, and the percentage of eIF4E2 or eIF4E present in monosome and polysome fractions relative to the total signal was calculated.

RNA Isolation and quantitative RT-PCR

RNA was extracted from polysome fractions and qRT-PCR performed for Fig. 4A-B and E as previously described [17]. RNA extracted from cells for Fig. 4D and Fig. 5B using RiboZol™ as per manufacturer's instructions. RNA (4 μg) was reverse transcribed using the high-capacity cDNA reverse transcription kit (Applied Biosystems). Primer sequences used (5'-3'): *CITED2*, CCT AAT GGG CGA GCA CAT ACA (forward) and CGT TCG TGG CAT TCA TGTT (reverse); *EEF2*, Forward TTC AAG TCA TTC TCC GAG A and Reverse AGA CAC GCT TCA CTG ATA; *EGFR*, GGA GAA CTG CCA GAA ACT GAC (forward) and GGG GTT CAC ATC CAT CTG (reverse); *EPO*, TGG AAG AGG ATG GAG GTC GG (forward) and AGA GTG GTG AGG CTG CGA A (reverse); *IGFBP3*, GCG CCA GGA AAT GCT AGT G (forward) and AAC TTG GGA TCA GAC ACC CG (reverse); *IGF1R*, CCA TTC TCA TGC CTT GGT CT (forward) and TGC AAG TTC TGG TTG TCG AG (reverse); *GAPDH*, GTC AAG GCT GAG AAC GGG A (forward) and CAA ATG AGC CCC AGC CTT C (reverse); *HSP90AB1*, TGT CCC TCA TCA TCA ATA CC (forward) and TCT TTA CCA CTG TCC AAC TT (reverse); *ITPR1*, CGG AGC AGG GTA TTG GAA CA (forward) and GGT CCA CTG AGG GCT GAA AC (reverse); *LOXL2*, CCC CCT GGA GAC TAC CTG TT (forward), GGA ACC ACC TAT GTG GCA GT (reverse); *OCT4*, GAT GTG GTC CGA GTG TGG TTC (forward) and TTG ATC GCT TGC CCT TCT G (reverse); *RPLP0*, AAC ATC TCC CCC TTC TCC (forward) and CCA GGA AGC GAG AAT GC (reverse); RPL13A, CAT AGG AAG CTG GGA GCA AG (forward) and GCC CTC CAA TCA GTC TTC TG (reverse). Relative fold change in expression was calculated using the ΔΔCT method, and transcript levels were normalized to *RPLP0* and either *RPL13A* or *GAPDH*.

Immunoprecipitation and vectors

Exogenous expression vectors used: FLAG-GFP-HIF-2α in a pAdlox backbone was a gift from Dr. Stephen Lee (Miami), HA-HIF1alpha-pcDNA3 was a gift from William Kaelin (Addgene plasmid # 18949; http://n2t.net/addgene:18949; RRID:Addgene_18949), and FLAG-eIF4E2 was a gift from Dong-Er Zhang (Addgene plasmid # 17342 ; http://n2t.net/addgene:17342 ; RRID:Addgene_17342). Control vectors were of the same backbone and tag without a gene insert. Cells were transfected with 4 μg DNA complexed with 20 μg polyethylenamine (PEI) diluted in 600 μL of lactate buffered saline (20 mM sodium lactate and 150 mM NaCl, pH 4.0). The DNA/PEI complexes were diluted in 2.4 mL DMEM without FBS or antibiotics and added to cells at 37 °C for 8 h followed by replenishing with complete media. Cells were lysed after 48 h in 200 μL lysis buffer [10 mM Tris-HCl (pH 7.4), 150 mM NaCl, 0.5 mM EDTA, 0.5% NP-40, 1X protease inhibitor cocktail (New England Biolabs)]. Lysates were centrifuged at 12,000 rpm for 10 min at 4 °C and diluted with 500 μL of dilution buffer [10 mM Tris-HCl (pH 7.4), 150 mM NaCl, 0.5 mM EDTA, 1X protease inhibitor cocktail]. Protein (1 mg/mL) was incubated with 25 μL of GFP-Trap magnetic micro beads (ChromoTek), or anti-FLAG M2 magnetic beads (Sigma), or anti-HA magnetic beads (Pierce). Only GFP-Trap required pre-blocking with 3% BSA in TBS [50 mM Tris, 150 mM NaCl, pH 7.4] and washed as per the manufacturer's instructions. Immunoprecipitation was carried out for 1 h at 4 °C with rotation. The GFP beads were washed four times with a more stringent wash buffer [10 mM Tris-HCl (pH 7.4), 500 mM NaCl, 0.5 mM EDTA, 0.1% NP-40] while FLAG and HA beads were washed four times with TBS. Proteins were eluted at 95 °C in 1X Laemmli sample buffer. Whole cell lysate (25 μg) was used as the input.

Analysis of Cap-Binding Proteins

Performed as previously described [39]. The eIF4E2 signal in input and cap-elution lanes was quantified by densitometry using Bio-Rad Image Lab software. The eIF4E2 signal in the DDX28 knockdown cap-elution lane relative to control was normalized to the eIF4E2 input signal ratio.

Cellular fractionation

After 24h of hypoxia, cells were lysed in 400 µL harvest buffer [10 mM HEPES, 50 mM NaCl, 500 mM sucrose, 0.1 mM EDTA, 10 mM DTT, 2 mM NaF, 0.5% Triton-X100, 1X protease inhibitor cocktail]. Lysates were centrifuged at 8000 rpm for 10 min at 4 °C to pellet nuclei. The supernatant was collected as the cytoplasmic fraction and the nuclear pellet was washed twice with 800 µL nuclear wash buffer [10 mM HEPES, 10 mM KCl, 0.1 mM EDTA, 0.1 mM EGTA, 10 mM DTT, 2 mM NaF, 1X protease inhibitor cocktail] centrifuging at 13,000 rpm at 4 °C for 5 and 10 min following washes. The nuclear pellet was resuspended in 400 µL RIPA buffer [20 mM Tris-HCl (pH 7.5), 10 mM NaCl, 1% NP-40, 0.1% SDS, 0.5% sodium deoxycholate, 1 mM EDTA, 10 mM DTT, 2 mM NaF, 1X protease inhibitor cocktail] and rotated at 4 °C for 15 min. Insoluble proteins were pelleted by centrifugation at 13,000 rpm for 10 min at 4 °C and the supernatant was collected as the nuclear fraction. Equal volumes of cytoplasmic and nuclear samples were mixed with 1X Laemmli sample buffer and boiled at 95 °C for 90 sec for western blot analysis.

Viability assay

For each indicated time point, 10,000 cells per well were plated in triplicate in a 24-well plate. The following day (day 0), cells were incubated at their indicated oxygen concentrations, and following each 24 h increment, cells were washed once with PBS and stained with 400 µL of 1% crystal violet solution prepared in 20% methanol, with gentle rocking for 20 min at room

temperature. Cells were gently washed with water to remove excess stain. Plates were air-dried overnight, and 400 µL of 10 % acetic acid was added to each well and incubated on a shaker for 20 min at room temperature for de-staining. The absorbance at 595 nm was measured using the ThermoMax microplate reader (Molecular Devices).

Cell proliferation assay

Cells (250,000) were seeded on coverslips and incubated at their indicated oxygen concentrations for 24 h prior to treatment with 10 µmol/l bromodeoxyuridine (BrdU) cell proliferation labeling reagent (Sigma) for 1 h. Cells were washed with PBS and fixed in cold methanol for 10 min. Excess methanol was removed by washing for 5 min with PBS, and coverslips were incubated with 1:100 primary anti-bromodeoxyuridine antibody (RPN202; GE Healthcare) in the dark for 1 h. Coverslips were washed three times for 5 min with PBS and incubated with 2 µg/mL goat anti-mouse Alexa Fluor 555 secondary antibody (Invitrogen,), in the dark for 1 h at 37 °C. Cells were counterstained with Hoechst (1 µg/mL) for 5 min, and coverslips were mounted on microscope slides using ProLong Gold antifade reagent (Invitrogen). Cells were imaged with the Nikon eclipse Ti-S inverted microscope. An average of 200 cells were assessed for positive BrdU labeling per biological replicate.

Statistical analyses

Results are expressed as means ± standard error of the mean (s.e.m) of at least three independent experiments. Experimental data were tested using unpaired two-tailed Student's t-test when only two means were compared, or a one-way ANOVA followed by Tukey's HSD test when three or more means were compared. $P < 0.05$ was considered statistically significant using GraphPad Prism.

AUTHOR CONTRIBUTIONS

SLE, OB, and EJS performed experiments. SLE and JU planned experiments, analyzed data and wrote the manuscript. JU designed the study and provided all the resources.

ACKNOWLEDGEMENTS

This work was funded by the Natural Sciences and Engineering Council of Canada (NSERC) grant number 04807 to J.U. S.L.E. was supported by the NSERC Canada Graduate Scholarships-Master's (CGS M).

REFERENCES

1. Semenza, G. L. (2011) Oxygen sensing, homeostasis, and disease, *N Engl J Med.* **365**, 537-47.
2. Dunwoodie, S. L. (2009) The role of hypoxia in development of the Mammalian embryo, *Dev Cell.* **17**, 755-73.
3. Simon, M. C. & Keith, B. (2008) The role of oxygen availability in embryonic development and stem cell function, *Nat Rev Mol Cell Biol.* **9**, 285-96.
4. Semenza, G. L. (2000) HIF-1: mediator of physiological and pathophysiological responses to hypoxia, *J Appl Physiol (1985).* **88**, 1474-80.
5. Withington, S. L., Scott, A. N., Saunders, D. N., Lopes Floro, K., Preis, J. I., Michalicek, J., Maclean, K., Sparrow, D. B., Barbera, J. P. & Dunwoodie, S. L. (2006) Loss of Cited2 affects trophoblast formation and vascularization of the mouse placenta, *Dev Biol.* **294**, 67-82.
6. Amarilio, R., Viukov, S. V., Sharir, A., Eshkar-Oren, I., Johnson, R. S. & Zelzer, E. (2007) HIF1alpha regulation of Sox9 is necessary to maintain differentiation of hypoxic prechondrogenic cells during early skeletogenesis, *Development.* **134**, 3917-28.
7. Jogi, A., Ora, I., Nilsson, H., Lindeheim, A., Makino, Y., Poellinger, L., Axelson, H. & Pahlman, S. (2002) Hypoxia alters gene expression in human neuroblastoma cells toward an immature and neural crest-like phenotype, *Proc Natl Acad Sci U S A.* **99**, 7021-6.
8. Licht, A. H., Muller-Holtkamp, F., Flamme, I. & Breier, G. (2006) Inhibition of hypoxia-inducible factor activity in endothelial cells disrupts embryonic cardiovascular development, *Blood.* **107**, 584-90.
9. Watson, E. D. & Cross, J. C. (2005) Development of structures and transport functions in the mouse placenta, *Physiology (Bethesda).* **20**, 180-93.
10. Yun, Z., Maecker, H. L., Johnson, R. S. & Giaccia, A. J. (2002) Inhibition of PPAR gamma 2 gene expression by the HIF-1-regulated gene DEC1/Stra13: a mechanism for regulation of adipogenesis by hypoxia, *Dev Cell.* **2**, 331-41.
11. Majmundar, A. J., Wong, W. J. & Simon, M. C. (2010) Hypoxia-inducible factors and the response to hypoxic stress, *Mol Cell.* **40**, 294-309.
12. Semenza, G. L. (2012) Hypoxia-inducible factors: mediators of cancer progression and targets for cancer therapy, *Trends Pharmacol Sci.* **33**, 207-14.

13. Downes, N. L., Laham-Karam, N., Kaikkonen, M. U. & Yla-Herttuala, S. (2018) Differential but Complementary HIF1alpha and HIF2alpha Transcriptional Regulation, *Mol Ther.* **26**, 1735-1745.
14. Lin, Q., Cong, X. & Yun, Z. (2011) Differential hypoxic regulation of hypoxia-inducible factors 1alpha and 2alpha, *Mol Cancer Res.* **9**, 757-65.
15. Talks, K. L., Turley, H., Gatter, K. C., Maxwell, P. H., Pugh, C. W., Ratcliffe, P. J. & Harris, A. L. (2000) The expression and distribution of the hypoxia-inducible factors HIF-1alpha and HIF-2alpha in normal human tissues, cancers, and tumor-associated macrophages, *Am J Pathol.* **157**, 411-21.
16. Uniacke, J., Holterman, C. E., Lachance, G., Franovic, A., Jacob, M. D., Fabian, M. R., Payette, J., Holcik, M., Pause, A. & Lee, S. (2012) An oxygen-regulated switch in the protein synthesis machinery, *Nature.* **486**, 126-9.
17. Timpano, S. & Uniacke, J. (2016) Human Cells Cultured under Physiological Oxygen Utilize Two Cap-binding Proteins to recruit Distinct mRNAs for Translation, *J Biol Chem.* **291**, 10772-82.
18. Brugarolas, J., Lei, K., Hurley, R. L., Manning, B. D., Reiling, J. H., Hafen, E., Witters, L. A., Ellisen, L. W. & Kaelin, W. G., Jr. (2004) Regulation of mTOR function in response to hypoxia by REDD1 and the TSC1/TSC2 tumor suppressor complex, *Genes Dev.* **18**, 2893-904.
19. Connolly, E., Braunstein, S., Formenti, S. & Schneider, R. J. (2006) Hypoxia inhibits protein synthesis through a 4E-BP1 and elongation factor 2 kinase pathway controlled by mTOR and uncoupled in breast cancer cells, *Mol Cell Biol.* **26**, 3955-65.
20. DeYoung, M. P., Horak, P., Sofer, A., Sgroi, D. & Ellisen, L. W. (2008) Hypoxia regulates TSC1/2-mTOR signaling and tumor suppression through REDD1-mediated 14-3-3 shuttling, *Genes Dev.* **22**, 239-51.
21. Liu, L., Cash, T. P., Jones, R. G., Keith, B., Thompson, C. B. & Simon, M. C. (2006) Hypoxia-induced energy stress regulates mRNA translation and cell growth, *Mol Cell.* **21**, 521-31.
22. Ho, J. J. D., Wang, M., Audas, T. E., Kwon, D., Carlsson, S. K., Timpano, S., Evagelou, S. L., Brothers, S., Gonzalgo, M. L., Krieger, J. R., Chen, S., Uniacke, J. & Lee, S. (2016) Systemic Reprogramming of Translation Efficiencies on Oxygen Stimulus, *Cell Rep.* **14**, 1293-1300.
23. Morita, M., Ler, L. W., Fabian, M. R., Siddiqui, N., Mullin, M., Henderson, V. C., Alain, T., Fonseca, B. D., Karashchuk, G., Bennett, C. F., Kabuta, T., Higashi, S., Larsson, O., Topisirovic, I., Smith, R. J., Gingras, A. C. & Sonenberg, N. (2012) A novel 4EHP-GIGYF2 translational repressor complex is essential for mammalian development, *Mol Cell Biol.* **32**, 3585-93.
24. Kelly, N. J., Varga, J. F. A., Specker, E. J., Romeo, C. M., Coomber, B. L. & Uniacke, J. (2018) Hypoxia activates cadherin-22 synthesis via eIF4E2 to drive cancer cell migration, invasion and adhesion, *Oncogene.* **37**, 651-662.
25. Uniacke, J., Perera, J. K., Lachance, G., Francisco, C. B. & Lee, S. (2014) Cancer cells exploit eIF4E2-directed synthesis of hypoxia response proteins to drive tumor progression, *Cancer Res.* **74**, 1379-89.
26. Valgardsdottir, R., Brede, G., Eide, L. G., Frengen, E. & Prydz, H. (2001) Cloning and characterization of MDDX28, a putative dead-box helicase with mitochondrial and nuclear localization, *J Biol Chem.* **276**, 32056-63.
27. Antonicka, H. & Shoubridge, E. A. (2015) Mitochondrial RNA Granules Are Centers for Posttranscriptional RNA Processing and Ribosome Biogenesis, *Cell Rep.*

28. Tu, Y. T. & Barrientos, A. (2015) The Human Mitochondrial DEAD-Box Protein DDX28 Resides in RNA Granules and Functions in Mitoribosome Assembly, *Cell Rep*.
29. Bousquet, P. A., Sandvik, J. A., Arntzen, M. O., Jeppesen Edin, N. F., Christoffersen, S., Krengel, U., Pettersen, E. O. & Thiede, B. (2015) Hypoxia Strongly Affects Mitochondrial Ribosomal Proteins and Translocases, as Shown by Quantitative Proteomics of HeLa Cells, *Int J Proteomics.* **2015**, 678527.
30. Volpon, L., Osborne, M. J., Topisirovic, I., Siddiqui, N. & Borden, K. L. (2006) Cap-free structure of eIF4E suggests a basis for conformational regulation by its ligands, *EMBO J.* **25**, 5138-49.
31. Thoreen, C. C., Chantranupong, L., Keys, H. R., Wang, T., Gray, N. S. & Sabatini, D. M. (2012) A unifying model for mTORC1-mediated regulation of mRNA translation, *Nature.* **485**, 109-13.
32. Aprelikova, O., Wood, M., Tackett, S., Chandramouli, G. V. & Barrett, J. C. (2006) Role of ETS transcription factors in the hypoxia-inducible factor-2 target gene selection, *Cancer Res.* **66**, 5641-7.
33. Elvidge, G. P., Glenny, L., Appelhoff, R. J., Ratcliffe, P. J., Ragoussis, J. & Gleadle, J. M. (2006) Concordant regulation of gene expression by hypoxia and 2-oxoglutarate-dependent dioxygenase inhibition: the role of HIF-1alpha, HIF-2alpha, and other pathways, *J Biol Chem.* **281**, 15215-26.
34. Hu, C. J., Sataur, A., Wang, L., Chen, H. & Simon, M. C. (2007) The N-terminal transactivation domain confers target gene specificity of hypoxia-inducible factors HIF-1alpha and HIF-2alpha, *Mol Biol Cell.* **18**, 4528-42.
35. Isono, T., Chano, T., Yoshida, T., Kageyama, S., Kawauchi, A., Suzaki, M. & Yuasa, T. (2016) Hydroxyl-HIF2-alpha is potential therapeutic target for renal cell carcinomas, *Am J Cancer Res.* **6**, 2263-2276.
36. Yi, T., Papadopoulos, E., Hagner, P. R. & Wagner, G. (2013) Hypoxia-inducible factor-1alpha (HIF-1alpha) promotes cap-dependent translation of selective mRNAs through up-regulating initiation factor eIF4E1 in breast cancer cells under hypoxia conditions, *J Biol Chem.* **288**, 18732-42.
37. Okumura, F., Zou, W. & Zhang, D. E. (2007) ISG15 modification of the eIF4E cognate 4EHP enhances cap structure-binding activity of 4EHP, *Genes Dev.* **21**, 255-60.
38. Melanson, G., Timpano, S. & Uniacke, J. (2017) The eIF4E2-Directed Hypoxic Cap-Dependent Translation Machinery Reveals Novel Therapeutic Potential for Cancer Treatment, *Oxid Med Cell Longev.* **2017**, 6098107.
39. Timpano, S., Melanson, G., Evagelou, S. L., Guild, B. D., Specker, E. J. & Uniacke, J. (2016) Analysis of Cap-binding Proteins in Human Cells Exposed to Physiological Oxygen Conditions, *J Vis Exp*.
40. Kuehn, B. M. (2010) Genomics illuminates a deadly brain cancer, *JAMA.* **303**, 925-7.
41. Yarden, Y. & Sliwkowski, M. X. (2001) Untangling the ErbB signalling network, *Nat Rev Mol Cell Biol.* **2**, 127-37.
42. Uhlen, M., Zhang, C., Lee, S., Sjostedt, E., Fagerberg, L., Bidkhori, G., Benfeitas, R., Arif, M., Liu, Z., Edfors, F., Sanli, K., von Feilitzen, K., Oksvold, P., Lundberg, E., Hober, S., Nilsson, P., Mattsson, J., Schwenk, J. M., Brunnstrom, H., Glimelius, B., Sjoblom, T., Edqvist, P. H., Djureinovic, D., Micke, P., Lindskog, C., Mardinoglu, A. & Ponten, F. (2017) A pathology atlas of the human cancer transcriptome, *Science.* **357**.

506 43. Razafinjatovo, C., Bihr, S., Mischo, A., Vogl, U., Schmidinger, M., Moch, H. & Schraml, P.
507 (2016) Characterization of VHL missense mutations in sporadic clear cell renal cell carcinoma:
508 hotspots, affected binding domains, functional impact on pVHL and therapeutic relevance, *BMC*
509 *Cancer*. **16**, 638.
510
511 **FIGURE LEGENDS**

512 **Figure 1. DDX28 interacts with HIF-2α, but not HIF-1α or eIF4E2.** (A) Western blot of total
513 HIF-2α and DDX28 protein levels in normoxia (21% O_2) and hypoxia (1% O_2). GAPDH used as
514 a loading control. (B) Western blot of DDX28 and HIF-2α (arrow, hypoxia-inducible lower
515 band) normoxic and hypoxic protein levels in control (Ctrl) cells stably expressing a non-
516 targeting shRNA or in cells stably expressing one of two shRNAs targeting DDX28 mRNA:
517 Knockdown (KD) 1 and KD2. Actin used as a loading control. (C) GFP co-immunoprecipitation
518 in hypoxic cells stably expressing FLAG-DDX28 and transfected with recombinant GFP-HIF-
519 2α. Cells transfected with no DNA (-) or GFP alone were used as controls. (D) FLAG co-
520 immunoprecipitation of recombinant FLAG-eIF4E2 from hypoxic cells co-transfected with HA-
521 HIF-2α. Cells transfected with empty FLAG vector used as control. (E) FLAG co-
522 immunoprecipitation in hypoxic cells stably expressing FLAG-DDX28 and transfected with
523 recombinant HA-HIF-1α. Cells transfected with empty FLAG vector used as control. SE, short
524 exposure; LE, long exposure. 25 μg of whole cell lysate was used as input. Experiments
525 performed in U87MG glioblastoma.

526 **Figure 2. Knockdown of DDX28 increases the cap-binding affinity of eIF4E2.** Western blot
527 and quantification of eIF4E2 capture with m^7GTP-bound agarose beads in cells stably expressing
528 one of two distinct shRNA sequences targeting DDX28 in 1% O_2 hypoxia (A-B) and 21% O_2
529 normoxia (C-D). 35 μg of whole cell lysate was used as the input. Ctrl, control cells stably
530 expressing non-targeting shRNA; KD1 and KD2, knockdown cells stably expressing one of two

distinct shRNA sequences targeting DDX28; LE, long exposure. Data ($n \geq 3$), mean ± s.e.m normalized to input. * represents $p < 0.05$ using one sample t-test against hypothetical mean ($\mu = 1$). Experiments performed in U87MG glioblastoma.

Figure 3. Knockdown of DDX28 increases polysome-associated eIF4E2 only in hypoxia. Polysomal distribution of DDX28, eIF4E2 and eIF4E protein measured by western blot in control cells stably expressing non-targeting shRNA in 21% O_2 normoxia (A) and 1% O_2 hypoxia (C) and in Knockdown (KD) cells stably expressing an shRNA targeting DDX28 in normoxia (B) and hypoxia (D). Ribosomal protein L5 (rpL5) used as a marker of protein integrity in each fraction. The eIF4E (E) or eIF4E2 (F) protein associated with polysomes (fractions 4-9) as a percentage of total protein (fractions 1-9) was quantified by densitometry. Data ($n = 3$), mean ± s.e.m. * represents $p < 0.05$ using one-way ANOVA and Tukey's HSD post-hoc test. Experiments performed in U87MG glioblastoma.

Figure 4. Depletion of DDX28 increases the polysome association of eIF4E2-dependent transcripts in hypoxia. The association of eIF4E2-dependent transcripts Epidermal Growth Factor Receptor (EGFR) and Insulin Like Growth Factor 1 Receptor (IGF1R) with polysomes (fractions 4-9 from Fig. 3) was measured relative to monosomes (fractions 1-3) by qRT-PCR in control cells expressing a non-targeting shRNA or Knockdown (KD) cells stably expressing an shRNA targeting DDX28 in 1% O_2 hypoxia (A) and 21% O_2 normoxia (B). Western blot of total EGFR, DDX28, and Actin protein levels (C) or qRT-PCR of total EGFR mRNA levels normalized to endogenous control genes RPLP0 and RPL13A (D) in hypoxic control cells or DDX28 KD cells. (E) The association of eIF4E-dependent transcripts Eukaryotic Translation Elongation Factor 2 (EEF2) and Heat Shock Protein 90 Alpha Family Class B Member 1

(HSP90ab1) with polysomes was measured relative to monosomes by qRT-PCR in control cells or DDX28 KD cells in hypoxia and normoxia. Data ($n \geq 3$), mean ± s.e.m. * represents $p < 0.05$ using unpaired two-sample t-test except in (D) a one-sample t-test against a hypothetical mean ($\mu = 1$).

Figure 5. Depletion of DDX28 in hypoxia increases cytoplasmic and nuclear HIF-2α levels, but not its nuclear activity. (A) Western blot of HIF-2α protein levels in cytoplasmic and nuclear fractions of control cells expressing a non-targeting shRNA or Knockdown (KD) cells stably expressing an shRNA targeting DDX28 in 1% O_2 hypoxia. Lamin a/c used as nuclear marker and α-tubulin as cytoplasmic marker. (B) The mRNA abundance of HIF-2α gene targets in hypoxia measured via qRT-PCR. Data ($n \geq 3$), mean ± s.e.m. represented as $\log_2$ (fold change) in DDX28 KD cells relative to control cells and normalized to endogenous control genes RPLP0 and RPL13A. * represents $p < 0.05$ using a one-sample t-test against hypothetical mean ($\mu = 0$). CITED2, Cbp/P300-Interacting Transactivator 2; EPO, Erythropoietin; IGFBP3, Insulin Like Growth Factor Binding Protein 3; ITPR1, inositol 1,4,5-trisphosphate receptor type 1; LOXL2, Lysyl Oxidase Like 2; OCT4, octamer-binding transcription factor 4. Experiments performed in U87MG glioblastoma.

Figure 6. DDX28 depletion causes an increase in cell viability and proliferation only in hypoxia. Viable cell counts were measured with crystal violet staining after 24 h, 48 h, and 72 h in 21% O_2 normoxia (A) and 1% O_2 hypoxia (B) for control cells expressing a non-targeting shRNA or Knockdown cells stably expressing one of two shRNAs targeting DDX28 (KD1 and KD2). All absolute cell count values were normalized to the number of cells present on day 0 for each individual independent experiment, representing the fold change in the number of cells at each time point relative to day 0. Proliferation was measured as % BrdU-positive control and

577 DDX28 KD cells via immunofluorescence after 24 h in normoxia (C) or hypoxia (D). Data (n ≥
578 3), mean ± s.e.m. * represents $p < 0.05$ using an unpaired two-sample t-test. Experiments
579 performed in U87MG glioblastoma.

580 **Figure 7. Model of HIF-2α regulation via DDX28.** (A) In situations of low DDX28 such as 1%
581 O_2 hypoxia or shRNA depletion of DDX28 in normoxia, HIF-2α becomes more stabilized and
582 shifts the balance toward complex formation with eIF4E2 and a higher affinity for the m^7GTP 5'
583 cap structure. This, along with the binding of known interactors eIF4G3, eIF4A and RBM4,
584 induces the translation of transcripts harboring RNA hypoxia response elements (rHRE) in their
585 3'UTR. (B) Steady-state or "normal" DDX28 levels observed in normoxia contribute to the
586 normoxic decrease in HIF-2α protein levels through binding with DDX28 and shifts the balance
587 away from the formation of an activating complex with eIF4E2, repressing this non-canonical
588 cap-dependent translation pathway. Since depleting DDX28 in hypoxia activates eIF4E2-
589 dependent translation even further, we propose that some DDX28 is required in hypoxia to
590 restrain this oncogenic pathway.

Figure 1

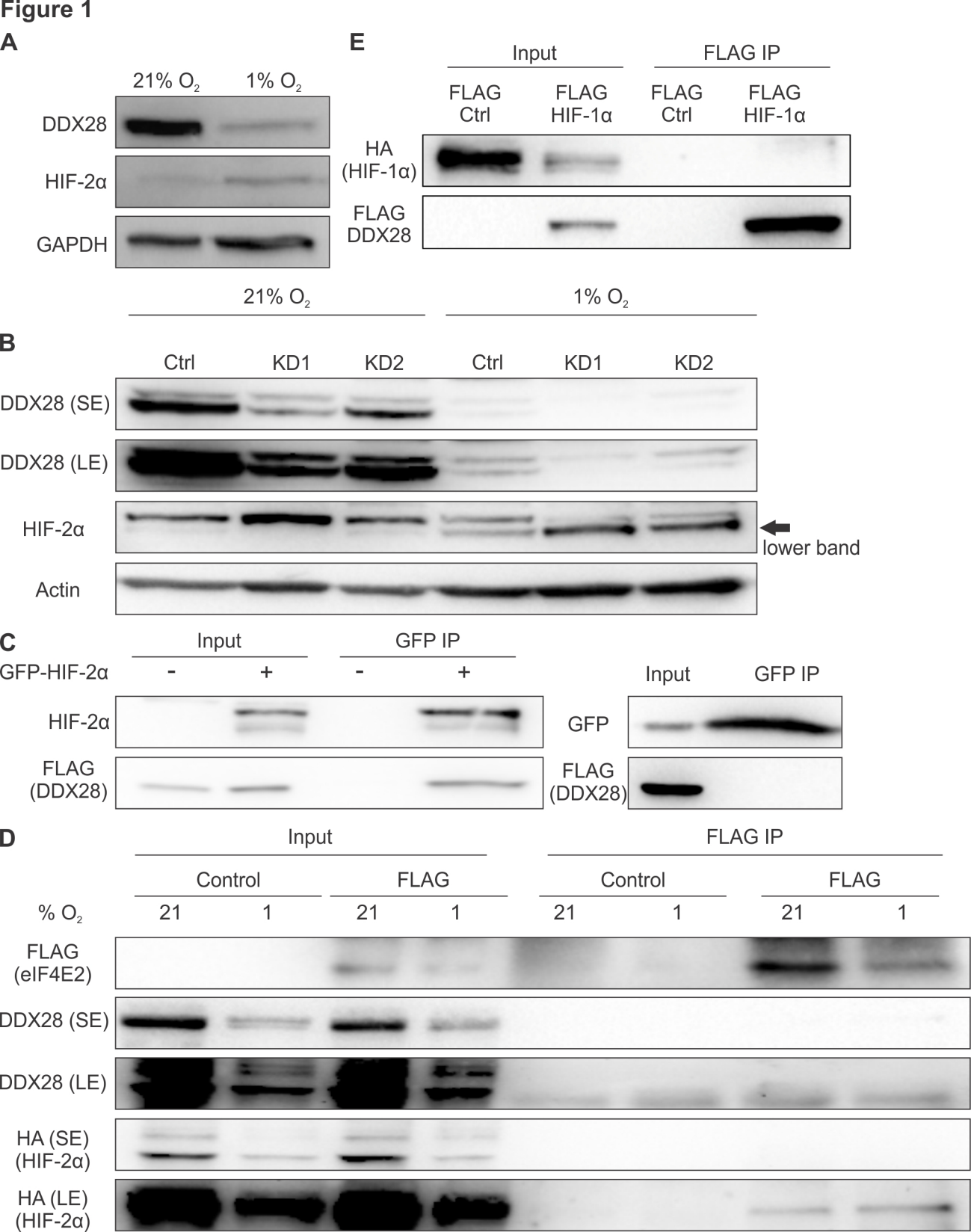
A
21% O2
1% O2
DDX28
HIF-2α
GAPDH
E
Input
FLAG IP
FLAG Ctrl
FLAG HIF-1α
FLAG Ctrl
FLAG HIF-1α
HA (HIF-1α)
FLAG DDX28
21% O2
1% O2
B
Ctrl
KD1
KD2
Ctrl
KD1
KD2
DDX28 (SE)
DDX28 (LE)
HIF-2α
lower band
Actin
C
Input
GFP IP
GFP-HIF-2α
-
+
-
+
HIF-2α
FLAG (DDX28)
Input
GFP IP
GFP
FLAG (DDX28)
D
Input
FLAG IP
Control
FLAG
Control
FLAG
% O2
21
1
21
1
21
1
21
1
FLAG (eIF4E2)
DDX28 (SE)
DDX28 (LE)
HA (SE) (HIF-2α)
HA (LE) (HIF-2α)

Figure 2

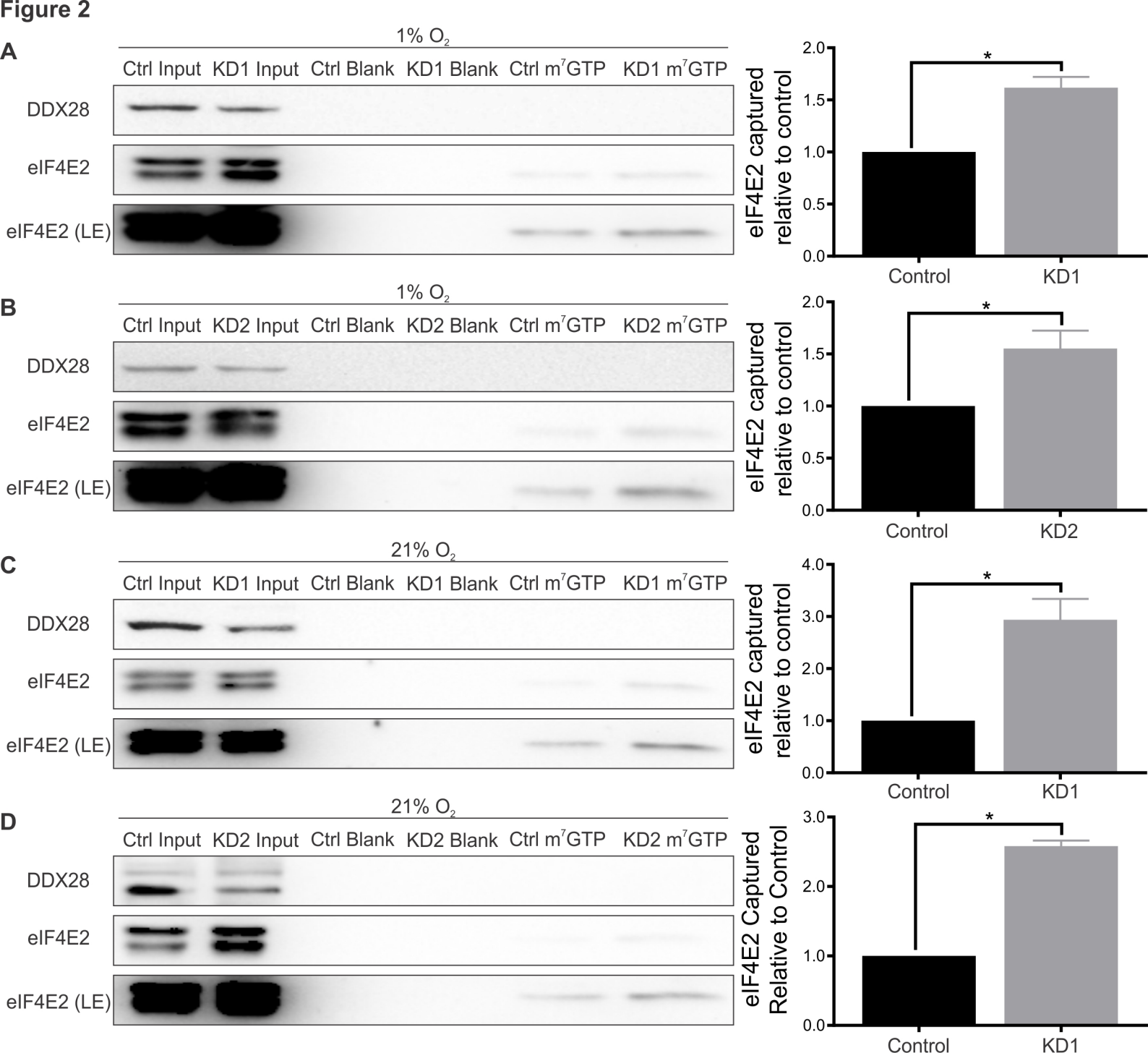
A
1% O2
Ctrl Input
KD1 Input
Ctrl Blank
KD1 Blank
Ctrl m7GTP
KD1 m7GTP
DDX28
eIF4E2
eIF4E2 (LE)
eIF4E2 captured relative to control
2.0
1.5
1.0
0.5
0.0
*
Control
KD1
B
1% O2
Ctrl Input
KD2 Input
Ctrl Blank
KD2 Blank
Ctrl m7GTP
KD2 m7GTP
DDX28
eIF4E2
eIF4E2 (LE)
eIF4E2 captured relative to control
2.0
1.5
1.0
0.5
0.0
*
Control
KD2
C
21% O2
Ctrl Input
KD1 Input
Ctrl Blank
KD1 Blank
Ctrl m7GTP
KD1 m7GTP
DDX28
eIF4E2
eIF4E2 (LE)
eIF4E2 captured relative to control
4.0
3.0
2.0
1.0
0.0
*
Control
KD1
D
21% O2
Ctrl Input
KD2 Input
Ctrl Blank
KD2 Blank
Ctrl m7GTP
KD2 m7GTP
DDX28
eIF4E2
eIF4E2 (LE)
eIF4E2 Captured Relative to Control
3.0
2.0
1.0
0.0
*
Control
KD1

Figure 3

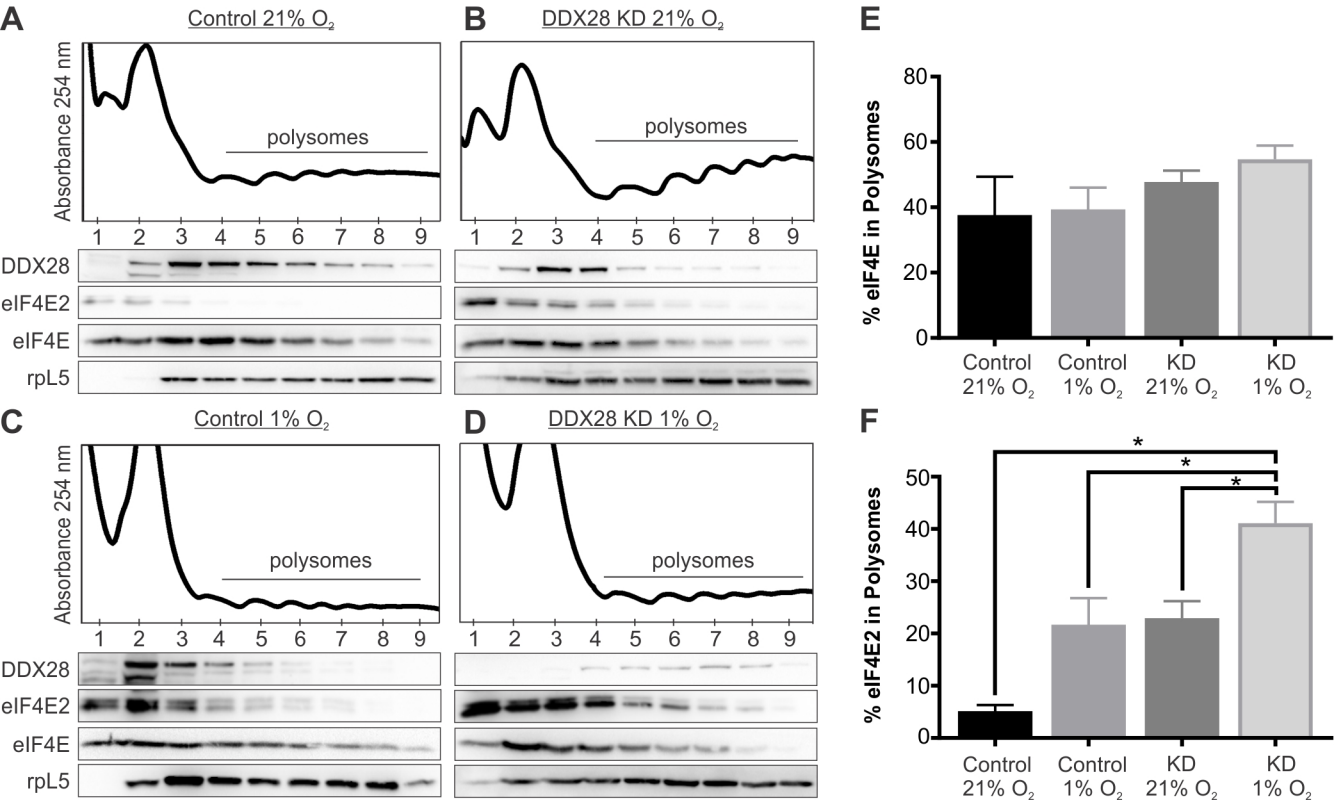
A
Control 21% O2
Absorbance 254 nm
polysomes
1 2 3 4 5 6 7 8 9
DDX28
eIF4E2
eIF4E
rpL5
B
DDX28 KD 21% O2
polysomes
C
Control 1% O2
D
DDX28 KD 1% O2
E
% eIF4E in Polysomes
80
60
40
20
0
Control 21% O2
Control 1% O2
KD 21% O2
KD 1% O2
F
% eIF4E2 in Polysomes
50
40
30
20
10
0
*

Figure 4

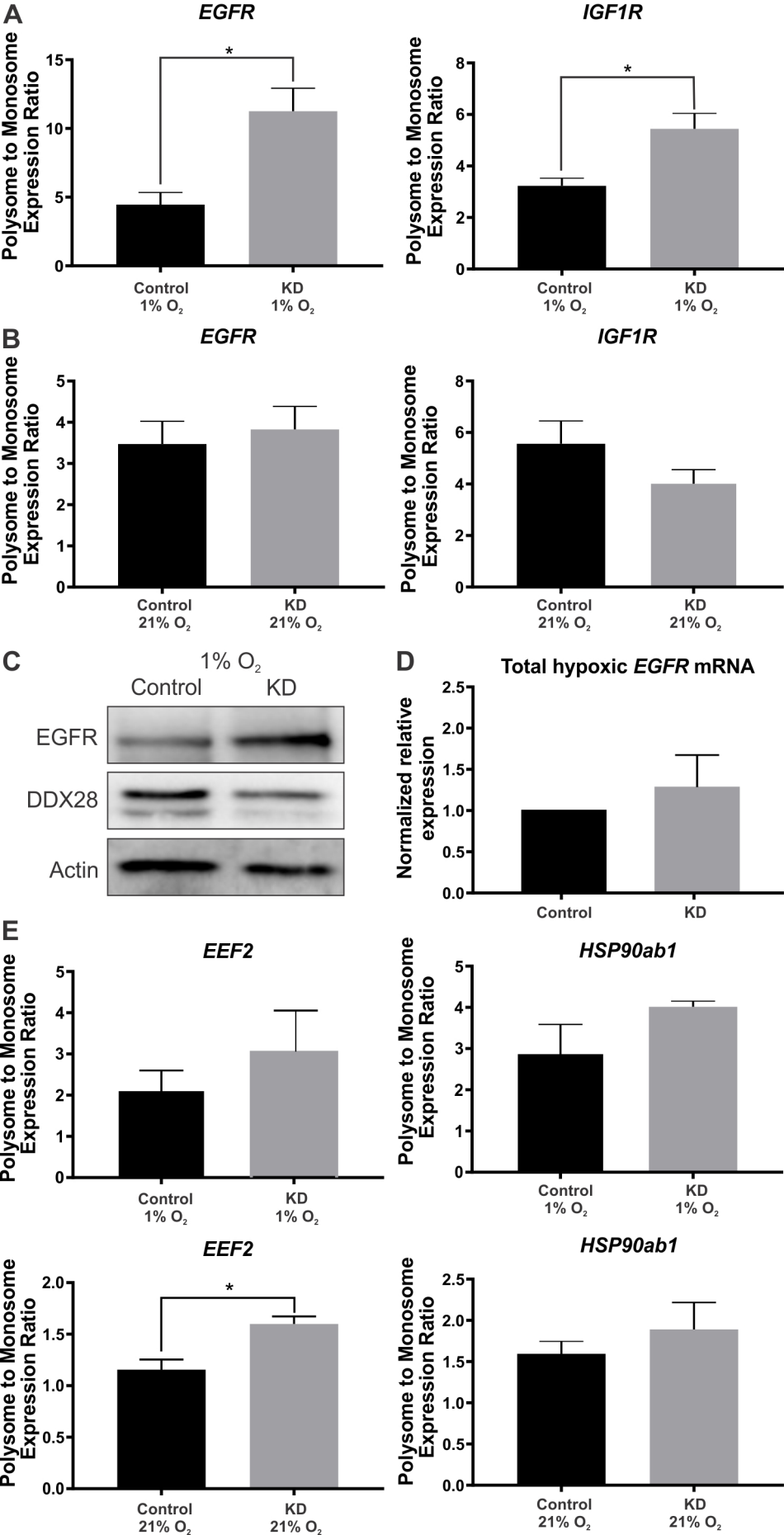
A
EGFR
IGF1R
Polysome to Monosome Expression Ratio
*
Control 1% O2
KD 1% O2
B
EGFR
IGF1R
Control 21% O2
KD 21% O2
C
1% O2
Control
KD
EGFR
DDX28
Actin
D
Total hypoxic EGFR mRNA
Normalized relative expression
E
EEF2
HSP90ab1

Figure 5

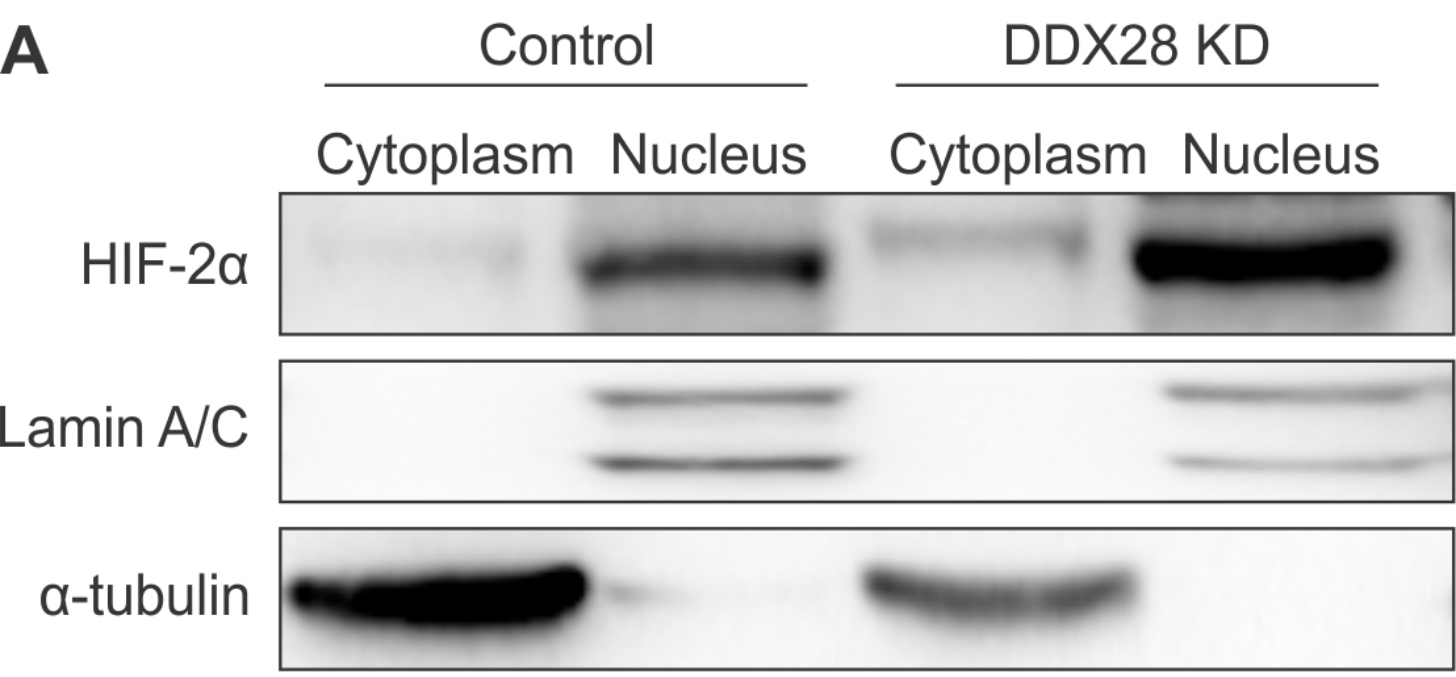
A
Control
DDX28 KD
Cytoplasm
Nucleus
Cytoplasm
Nucleus
HIF-2α
Lamin A/C
α-tubulin

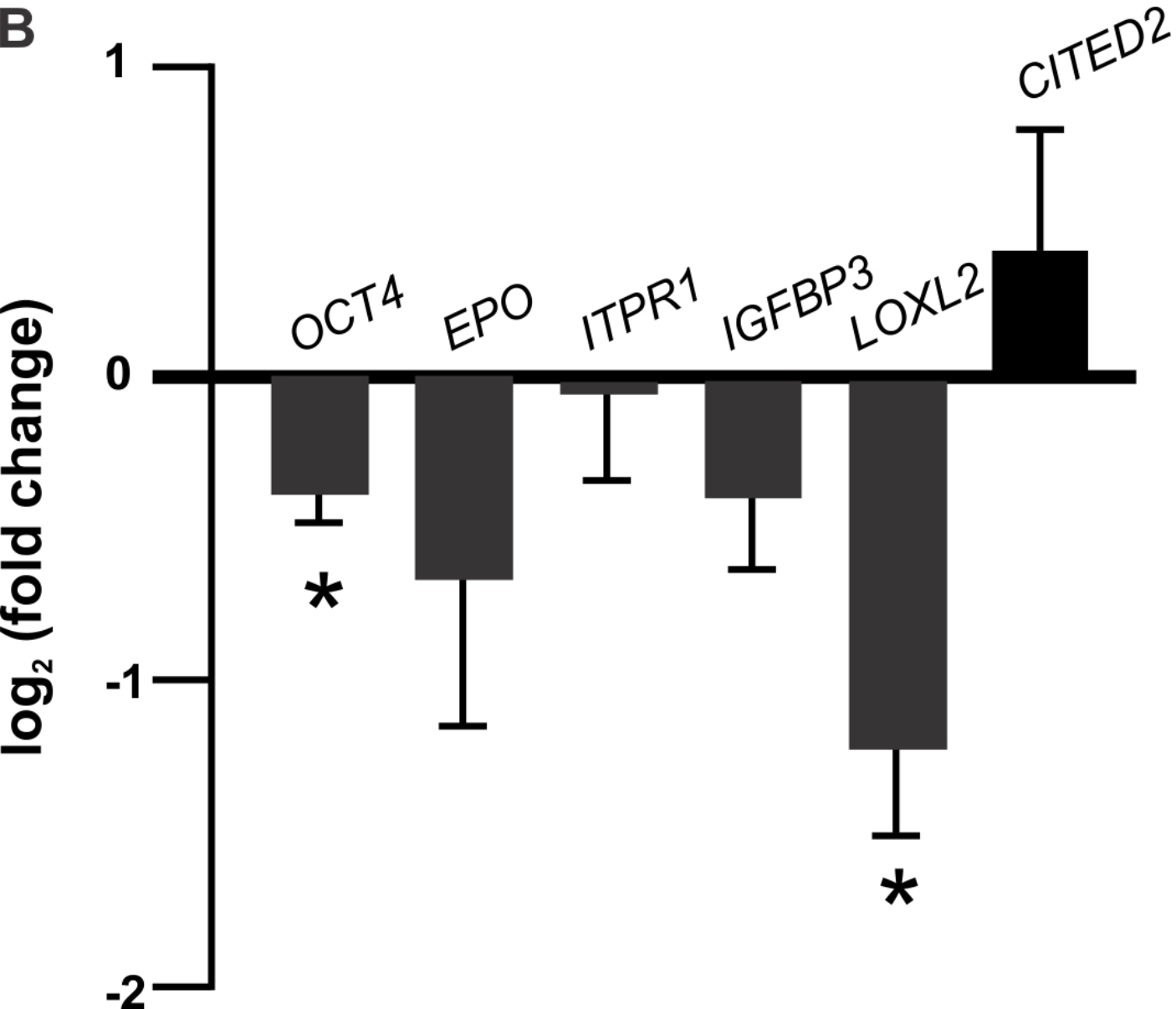
B
1
0
-1
-2
log2 (fold change)
OCT4
EPO
ITPR1
IGFBP3
LOXL2
CITED2
*
*

Figure 6

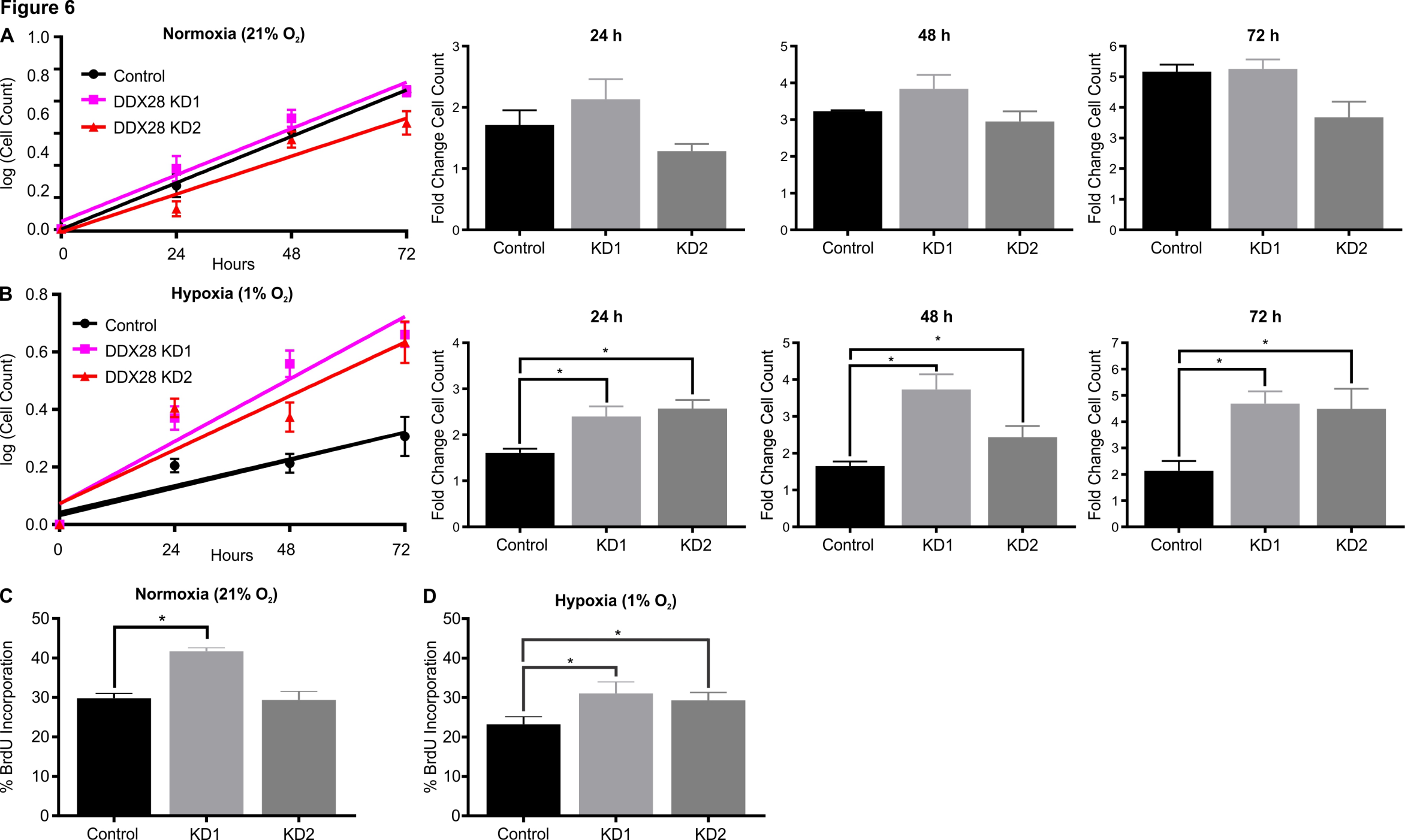
A
Normoxia (21% O2)
log (Cell Count)
Control
DDX28 KD1
DDX28 KD2
Hours
24 h
48 h
72 h
Fold Change Cell Count
Control
KD1
KD2
B
Hypoxia (1% O2)
C
Normoxia (21% O2)
% BrdU Incorporation
D
Hypoxia (1% O2)

Figure 7

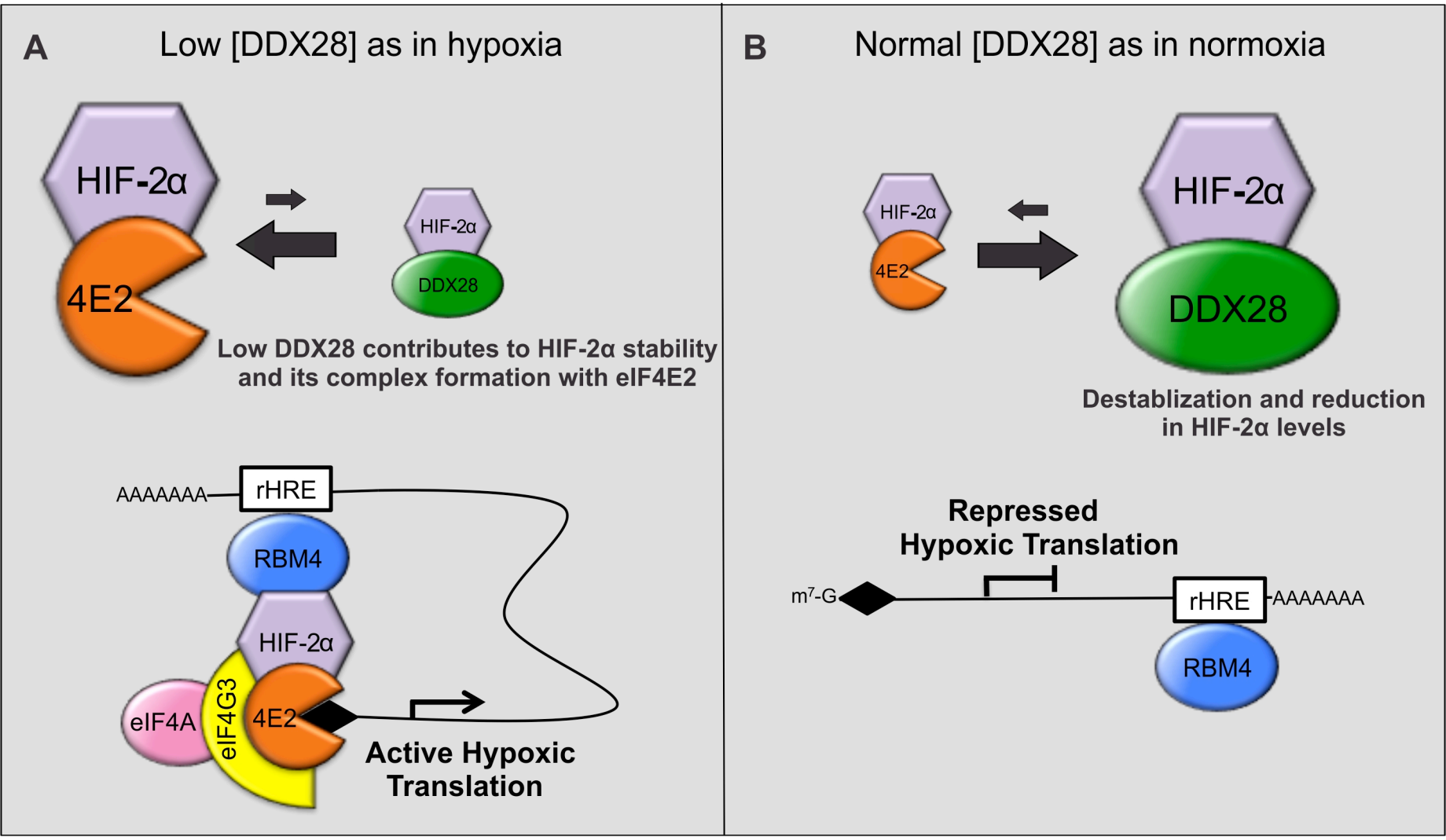
A
Low [DDX28] as in hypoxia
HIF-2α
4E2
HIF-2α
DDX28
Low DDX28 contributes to HIF-2α stability
and its complex formation with eIF4E2
AAAAAAA
rHRE
RBM4
HIF-2α
eIF4A
eIF4G3
4E2
Active Hypoxic
Translation
B
Normal [DDX28] as in normoxia
HIF-2α
4E2
HIF-2α
DDX28
Destablization and reduction
in HIF-2α levels
Repressed
Hypoxic Translation
m7-G
rHRE
AAAAAAA
RBM4